Geophysical Research Letters

RESEARCH LETTER
10.1029/2018GL077813

Key Points:
- MODIS-derived near-surface air and dew point temperatures exhibit no major errors or biases against ground observations across biomes
- The validated 5 km resolution, global, daily observations provide a wealth of global surface meteorological data for varied applications
- These results are among the first assessments of the reprocessed, crosstalk-corrected Collection 6.1 Terra MODIS data

Supporting Information:
- Supporting Information S1

Correspondence to:
J. B. Fisher,
jbfisher@jpl.nasa.gov

Citation:
Famiglietti, C. A., Fisher, J. B., Halverson, G., & Borbas, E. E. (2018). Global validation of MODIS near-surface air and dew point temperatures. *Geophysical Research Letters*, *45*, 7772–7780. https://doi.org/10.1029/2018GL077813

Received 6 MAR 2018
Accepted 5 APR 2018
Accepted article online 19 APR 2018
Published online 30 APR 2018

Global Validation of MODIS Near-Surface Air and Dew Point Temperatures

Caroline A. Famiglietti[1,2], Joshua B. Fisher[2], Gregory Halverson[2,3], and Eva E. Borbas[4]

[1]Department of Mathematics, University of California, Los Angeles, CA, USA, [2]Jet Propulsion Laboratory, California Institute of Technology, Pasadena, CA, USA, [3]Department of Geography and Environmental Studies, California State University, Northridge, CA, USA, [4]Cooperative Institute for Meteorological Satellite Studies, University of Wisconsin-Madison, Madison, WI, USA

Abstract This analysis is the first global validation of the Moderate Resolution Imaging Spectroradiometer (MODIS)-derived near-surface air temperature and dew point estimates, which both serve as crucial input data in models of energy, water, and carbon exchange between terrestrial ecosystems and the atmosphere. By hypsometrically interpolating the MOD07 Level-2 atmospheric profile product to surface pressure level, we obtained near-surface air temperature and dew point observations at 5 km pixel resolution. We compared these daily data, retrieved over a 14-year record, to corresponding measurements from 109 ground meteorological stations (FLUXNET). Our results show strong agreement between satellite and in situ near-surface air temperature measurements (R^2 = 0.89, root-mean-square error = 3.47°C, and bias = −0.19°C) and dew point observations (R^2 = 0.76, root-mean-square error = 5.04°C, and bias = 0.79°C) with insignificant differences in error across climate zones. This validation is among the earliest assessments of the reprocessed, crosstalk-corrected Collection 6.1 Terra MODIS data and provides support for widespread applications of near-surface atmospheric data.

Plain Language Summary Scientists often use complex models to study the Earth's land, water, and atmosphere. Most models require various types of data that describe different processes critical to climate. Two common ingredients in these models are air temperature and dew point temperature, the latter a measure of the moisture in the air, near the ground. Although weather stations can report the two temperatures at precise locations, satellites can make measurements that are uniformly distributed over the entire globe. For this reason, many models use satellite data, particularly those with moderate to fine resolution, to represent near-surface air temperature and dew point. One common source of such data is a product from the Moderate Resolution Imaging Spectroradiometer (MODIS) satellite instrument. Satellite data require comparison against ground measurements, and, until now, the uncertainties in near-surface air temperature and dew point from the MODIS product had not been thoroughly studied. In this analysis, we compared daily MODIS data over a 14-year record to corresponding measurements from over 100 ground meteorological stations worldwide. The high accuracy we uncovered will allow other scientists to confidently use near-surface air temperature and dew point estimates from the satellite product in their models.

1. Introduction

Near-surface air temperature (T_a) and dew point (T_d) are two key variables used to quantify the exchanges of energy, water, and carbon between the land surface and the atmosphere and serve as vital indicators of terrestrial environmental conditions worldwide (Penman, 1948; Sellers et al., 1997). Many global hydrological, climatological, and ecological models, including those of snow cover, solar radiation, and evapotranspiration, among others, rely on T_a and T_d (or a corresponding measure of humidity) as input data (Arnold et al., 1998; Brun et al., 1989; Hubbard et al., 2003; Rehman & Mohandes, 2008). Continuous measurements of both variables help characterize the atmospheric capacity for moisture as well as its evolution in space and time. The accuracy in estimation of the two temperatures is inherently linked to the resulting precision and implications of such models and is therefore essential in understanding their outputs.

Currently available data sets providing T_a and T_d vary in spatial resolution according to application. Ground meteorological stations from networks like FLUXNET, a global network of hundreds of micrometeorological flux measurement sites (Baldocchi et al., 2001), or those coalesced by the Climatic Research Unit (CRU), which collates climate data sets from thousands of globally distributed weather stations (Harris et al., 2014), provide point measurements of T_a and T_d equivalents at precise geographical locations. Low-resolution alternatives

include reanalyses such as the NCEP/NCAR Reanalysis (a joint project from the National Centers for Environmental Prediction and the National Center for Atmospheric Research; Kalnay et al., 1996); the Modern-Era Retrospective Analysis for Research and Applications, Version 2 (MERRA-2), from the National Aeronautics and Space Administration (NASA) Global Modeling and Assimilation Office (Gelaro et al., 2017); and the European Centre for Medium-Range Weather Forecasts Reanalysis (ERA; Dee et al., 2011), which provide assimilated climate observations on grids of ~200, ~50, and ~80 km, respectively, or the Atmospheric Infrared Sounder (AIRS) aboard NASA's Aqua Earth Observing System satellite, which generates daily soundings on a 50 km grid (Aumann et al., 2003). However, in contrast to the above sources, a key niche exists for moderate- to fine-resolution data (Wood et al., 2011). Notably, many global evapotranspiration algorithms, seeking to describe processes at scales of agricultural fields (e.g., 100–1,000 m) and heterogeneous forest shapes, require relatively fine-resolution remotely sensed forcing data (Kite & Droogers, 2000).

The MOD07 Level-2 atmospheric profile product from the Moderate Resolution Imaging Spectroradiometer (MODIS) aboard the Terra and Aqua satellites is one such moderate- to fine-resolution option, providing temperature and moisture profiles at 20 vertically distributed levels with 5 km pixel resolution when at least 20% of the radiances measured are cloud-free (King et al., 2003). The MODIS atmospheric temperature and moisture retrieval algorithms use a clear-sky synthetic regression that relies on a fast radiative transfer model with atmospheric characteristics derived from a data set of global radiosonde measures (Seemann et al., 2003), and the resulting data set has myriad applications that include the calculation of higher-level physical variables (Bisht et al., 2005; Wan et al., 2002) as well as atmospheric correction of optical imagery (Jiménez-Muñoz et al., 2010). Daily near-surface T_a and T_d observations can be extracted from the MOD07 product by hypsometrically interpolating to surface pressure level (Bisht & Bras, 2010; Verma et al., 2016), yielding global moderate- to fine-resolution distributions of T_a and T_d.

However, no robust, large-scale validation of the near-surface MOD07 temperature estimates has been performed, making the quality of the retrievals at the heights relevant for many modeling applications heretofore relatively unknown. The MODIS Atmospheric Profile Retrieval Algorithm Theoretical Basis Document noted that the MOD07 profiles are routinely compared to in situ radiosonde measurements as well as to soundings from AIRS and the National Oceanic and Atmospheric Administration's Geostationary Operational Environmental Satellite. The document also validated the MOD07 total precipitable water and total ozone products (Borbas et al., 2011). Some studies involving the two remotely sensed near-surface temperatures provided further validation. Bisht and Bras (2010) compared observed and MODIS-retrieved T_a and T_d measurements from the Southern Great Plains, USA, for one year. Zhu et al. (2017) also validated MOD07-derived retrievals against in situ observations in the Southern Great Plains region, as well as in the Qaidam Basin in China, but only for T_a. Kim and Hogue (2008) evaluated the T_a and T_d data from 2001 to 2004 at four U.S. study sites. A systematic global error assessment of the near-surface T_a and T_d retrievals, though, remains to be performed. Furthermore, many previous studies used Collection 5 Terra MODIS data, which do not include significant algorithm updates introduced in recent years with Collections 6 and 6.1 (such as changes to the radiative transfer model used in the retrieval algorithms, improvements to quality control processing, and the development of a linear crosstalk correction algorithm).

Ground meteorological measurement networks offer a critical opportunity for validating such near-surface, moderate- to fine-resolution remote sensing data as the MOD07-derived T_a and T_d. Relatively recent advancements in the collation and availability of such measurements have enabled large-scale validations that were previously not feasible. Although the temporal latency, ubiquity of missing values, or heterogeneity of processing and formatting standards of many meteorological station data inhibit their comparability with the daily MODIS measurements, the abundance and consistency of subhourly observations via FLUXNET make its data sets ideally suited to such analysis.

We therefore present the first comprehensive, global analysis of the two MODIS-derived daily near-surface temperature estimates against data from 109 FLUXNET sites across six continents and all major climate types. Our analysis leverages Terra MODIS data from Collection 6.1, which includes retrieval algorithm improvements intended to offset errors associated with electronic crosstalk in the long-wave photovoltaic bands (Wilson et al., 2016). Our study period spanned 14 years, from 2001 to 2014, and is motivated by the use of such data in other studies, resulting in a need to have a robust understanding and quantification of the error in these products at a global scale. A full characterization of the accuracies of these forcing data sets, including

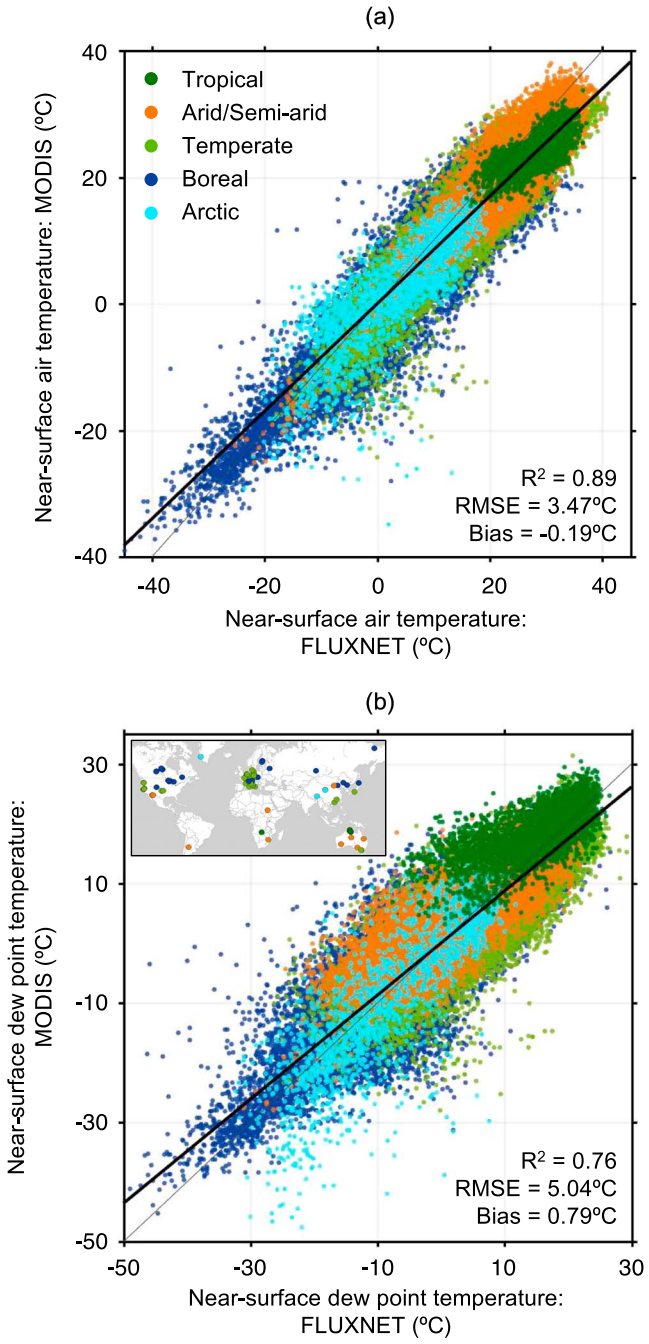

Figure 1. Correlations between remotely sensed and in situ (a) near-surface air temperature and (b) dew point were strong, and mean bias was minimal. Coloration of data points represents Köppen-Geiger climate classification, restricted to the five major groups. The colored circles within the map inset show the locations of the 109 FLUXNET sites included in this analysis, classified by climate type.

regional trends, provides valuable insights into data limitations and has vast implications for their impacts on many related modeling endeavors.

2. Methods

2.1. Hypsometric Interpolation of Temperature Profiles to Surface Level

Because MODIS possesses many spectral bands identical to those found on the High-resolution Infrared Radiation Sounder equipped aboard the National Oceanic and Atmospheric Administration TIROS Operational Vertical Sounder (TOVS), its infrared radiance measurements can be used to generate the vertical temperature and moisture profiles provided by the MOD07 Level-2 atmospheric profile product (Borbas et al., 2011). The retrieval algorithms are adapted from the International TOVS Processing Package and require data from MODIS channels 25 and 27–36, as well as from the MODIS cloud-mask product (MOD35 Level-2) and NCEP analysis of surface pressure (Borbas et al., 2011). We hypsometrically interpolated (i.e., by pressure level) these profiles, which correspond to atmospheric pressure levels, to surface level ($T_{surface}$) using the given surface pressure. This procedure yields estimates at approximately 2 m above the ground.

In each atmospheric column, we selected the temperature given at the nearest lower (T_{lower}) and higher (T_{upper}) altitudes and their corresponding pressures (P_{lower} and P_{upper}) for interpolation. We calculated the distance of the surface pressure level to the lower (Z_{lower}) or upper (Z_{upper}) atmospheric profile using the hypsometric equation with a gas constant of dry air (R) of 287.053 $J \cdot K^{-1} \cdot kg^{-1}$ and acceleration of gravity (g) of 9.8 m/s^2, where:

$$Z_{lower} = \frac{R}{g} * (T_{lower} + 273.16) * \log\left(\frac{P_{surface}}{P_{lower}}\right) \quad (1)$$

and

$$Z_{upper} = \frac{R}{g} * (T_{upper} + 273.16) * \log\left(\frac{P_{lower}}{P_{upper}}\right), \quad (2)$$

so that

$$T_{surface} = T_{lower} + (T_{lower} - T_{upper}) * \frac{Z_{upper}}{Z_{lower}}. \quad (3)$$

The MOD07 product provides explicit pixel confidence at two levels: "bad" or "best quality" (Hubanks, 2017). To avoid including invalid pixels, we excluded the lower confidence level from this analysis. Additionally, we considered no values of T_a lower than 233.0 K or greater than 353.0 K, no values of T_d lower than 213.0 K or greater than 353.0 K, and no values of either T_a or T_d exceeding two standard deviations from the mean of any 30-day period containing their date of retrieval, given data were reported on at least 15 days during that period. In each data set, 7.2% of all observations were eliminated.

2.2. FLUXNET Data Retrieval

We selected the set of MODIS land tiles covering the Earth's landmass as the target extent. We retrieved all daytime Collection 6.1 Terra swaths intersecting this extent from 2001 to 2014, processed them to near-surface meteorology, and resampled them by nearest neighbor to the sinusoidal MODIS land tiles. For each FLUXNET location (see map in Figure 1b; Table S1), we sampled the nearest 5 km pixel within the appropriate MODIS land tile for all available days. Finally, we temporally interpolated corresponding half-hourly FLUXNET

measurements to the precise time of Terra overpass for each day (approximately 10:30 a.m.), given MODIS assumed clear-sky conditions on that day.

For meteorological variables, the FLUXNET2015 data processing pipeline is concise, involving only a quality control step and a gap-filling and/or downscaling step that yields an alternative data set (Fluxdata, 2016). To minimize bias, our analyses included interpolations over only the directly measured T_a and vapor pressure deficit (VPD) observations, in accordance with quality information flags contained in the data product. We downloaded and processed all FLUXNET data available at the time of acquisition, and excluded sites from our analyses if either (i) MODIS data at that location were unavailable or (ii) excessive landscape heterogeneity made a site-to-pixel comparison inappropriate. The continental and climatic distributions of the 109 FLUXNET sites included in this study are summarized in Figure S2.

The FLUXNET humidity equivalent, VPD (hPa), was converted to T_d (°C) (Bolton, 1980):

$$T_d = \frac{243.5 \cdot \ln(\varphi)}{17.67 - \ln(\varphi)}, \tag{4}$$

where

$$\varphi = e^{\left(\frac{17.67 \cdot T_a}{T_a + 243.5}\right)} - \frac{\mathrm{VPD}}{6.112}. \tag{5}$$

2.3. Error Statistics

With the in situ observations as input, we fit a regression line through the origin to analyze MODIS performance. The root-mean-square error (RMSE) and bias are defined as follows:

$$\mathrm{RMSE} = \sqrt{\frac{\sum_{i=1}^{n}\left(T_i - \widehat{T}_i\right)^2}{n}} \tag{6}$$

$$\mathrm{Bias} = \frac{\sum_{i=1}^{n}\left(T_i - \widehat{T}_i\right)}{n} \tag{7}$$

where T_i is the ith remotely sensed temperature measurement, $\widehat{T}_i$ is the corresponding prediction via the regression line, and n is the total number of observations. Constraining our linear model to pass through the origin allowed us to clearly define biases in the MODIS retrievals while yielding insignificant changes (≈1%) in the R^2 and RMSE values observed from the unconstrained fit.

Using the same linear model, we created global maps of error propagation. For T_a and T_d separately, we binned all MODIS observations in each of the five major Köppen-Geiger climate types by degree Celsius and calculated the average percent RMSE with respect to the regression line in each climate-wise, degree-wise grouping. We then applied the appropriate RMSE result to each 5 km pixel containing an annual mean remotely sensed temperature.

3. Results

The MOD07-derived T_a and T_d estimates were overall high in accuracy. Both sets of daily observations showed strong agreement with the corresponding in situ measurements (R^2 = 0.89, RMSE = 3.47°C, and bias = −0.19°C in the T_a data set; R^2 = 0.76, RMSE = 5.04°C, and bias = 0.79°C in the T_d data set; Figures 1a and 1b). To examine trends in global error propagation, we partitioned all data points by the major Köppen-Geiger climate type of each retrieval location, which reflects the average atmospheric conditions encountered by the MODIS detectors (Peel et al., 2007). We also assessed subdivisions relating to elevation, International Geosphere-Biosphere Programme (IGBP) land cover classification (Loveland et al., 2009), plant functional type, probability of excessive cloud cover, and duration of ground site data availability, but these analyses did not reveal any additional information than those by climate zone (Figures S3a and S3b).

Although climate-wise performance variations appeared pronounced in Arctic regions for both T_a and T_d, no differences in RMSE or bias between climates were statistically significant at $p < 0.05$ (Figures 2a and 2b). This finding implies that MODIS performance is marked by natural relative disparities rather than systematically biased or low-quality observations. Dew point estimates generally fluctuated more in accuracy than T_a

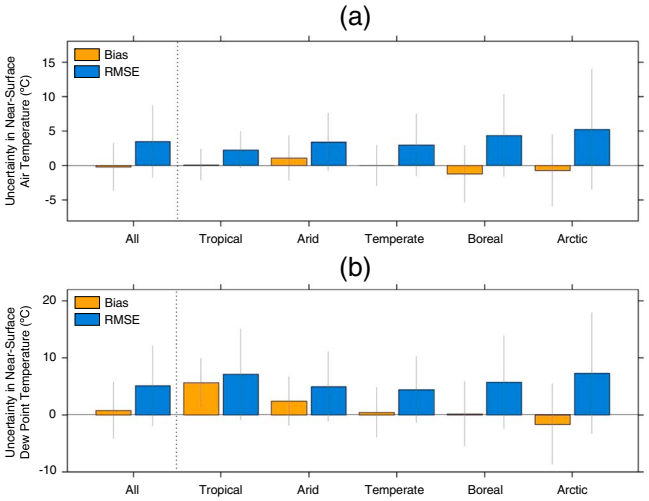

Figure 2. Uncertainties in MOD07-derived (a) near-surface air temperature and (b) dew point were low and insignificantly biased toward climate type. Orange represents mean bias; blue represents RMSE.

measurements overall as well as between corresponding climate types, likely due to the difficulty of satellite-based near-surface humidity estimation (Zhang et al., 2014).

For both MODIS temperature observations, the greatest variabilities in estimation accuracy were produced in regions of extreme temperature (Figures 3a–3d) and captured in fine detail (Figures S4a–S4d). In the Arctic and Sahara, at which the lowest and highest annual mean values, respectively, were measured by MODIS, T_a observations were more inconsistent than those in regions of moderate annual mean temperatures. Consequently, such errors were consistently low in the contiguous United States and Europe. The distribution of errors in T_d observations was analogous; accuracy of estimation in the Arctic and tropics varied most globally.

Atmospheric conditions in Arctic climates are perhaps most ill suited to the operational MODIS retrieval algorithm, which relies on several procedures including cloud detection (Borbas et al., 2011). Both temperature estimates showed inconsistencies, though insignificant, there. Seasonal variability may have additionally affected MODIS estimation accuracy. In particular, biases in T_a and T_d measurements were especially variable with season in Arctic regions, reaching maximum magnitudes in the winter (Figures S5a and S5b). Annual site-wise time series highlight this annual variability (Figure S6). However, although the seasonal variability in estimation accuracy at Sahel site SD-Dem was substantial, and the RMSE in high-extreme MODIS temperatures was reasonably large, a more complete understanding of error propagation and its causes in the Sahara, for T_a, and the Amazon, for T_d, is limited by the lack of ground meteorological station data available in both regions.

An ideal collection of ground sites would yield data nearly identical to the global distributions of T_a and T_d as measured by MODIS over the 14-year retrieval period. Accordingly, the limitations associated with the geographic clustering of our ground sites in temperate and boreal areas motivated us to resample the spatially-limited FLUXNET temperature distributions in accordance with the global variability of the entire land surface. These globally representative ground resamplings spanned both low and high extreme temperature ranges with higher probabilities than in the original FLUXNET distributions while constraining the contributions of the overly abundant near-median observations (Figures S7a–S7d). Statistical results from these secondary data sets showed improvements, though mostly minor ones, over those from the initial data sets. Notably, this procedure led R^2 to increase from 0.89 to 0.90 in the T_a data set and from 0.76 to 0.84 in the T_d data set (Figures S8a and S8b), which suggested that the simultaneous down-weighting of the more common intermediate temperatures (e.g., in North America and Europe) and up-weighting of the rarer extremes (e.g., in South America and Africa) did not significantly impact general MODIS performance metrics; in fact, linear correlations increased in strength. Furthermore, as contributions from data points in the more underrepresented climate zones (specifically the Arctic and tropics) became more pronounced, bias and RMSE in both resampled data sets consistently decreased, although no reduction exceeded 0.25°C.

4. Discussion

Errors calculated in this study may have originated from three possible sources: (i) the in situ measurements themselves; (ii) inconsistencies in the MODIS retrieval algorithm with possible associations to climate type, seasonality, or other factor(s), including electronic crosstalk in the long-wave infrared photovoltaic bands 27–30 (Wilson et al., 2016); or (iii) spatial heterogeneity within the 5 km pixels chosen for validation. Sufficient in situ data reliability was achieved by eliminating gap-filled or downscaled observations in favor of direct measurements, per the quality flags included in the FLUXNET data product. However, random errors within the ground data sets may have bypassed this filter.

Performance of the MODIS retrieval algorithm has been shown to vary with atmospheric conditions. In particular, the consistency of cloud detection by MODIS has been questioned, offering an explanation for the more variable estimation accuracy we observed in Arctic and tropical climates. A study by Østby et al. (2014) that explored the severe cloud contamination of MODIS land surface temperature estimates noted

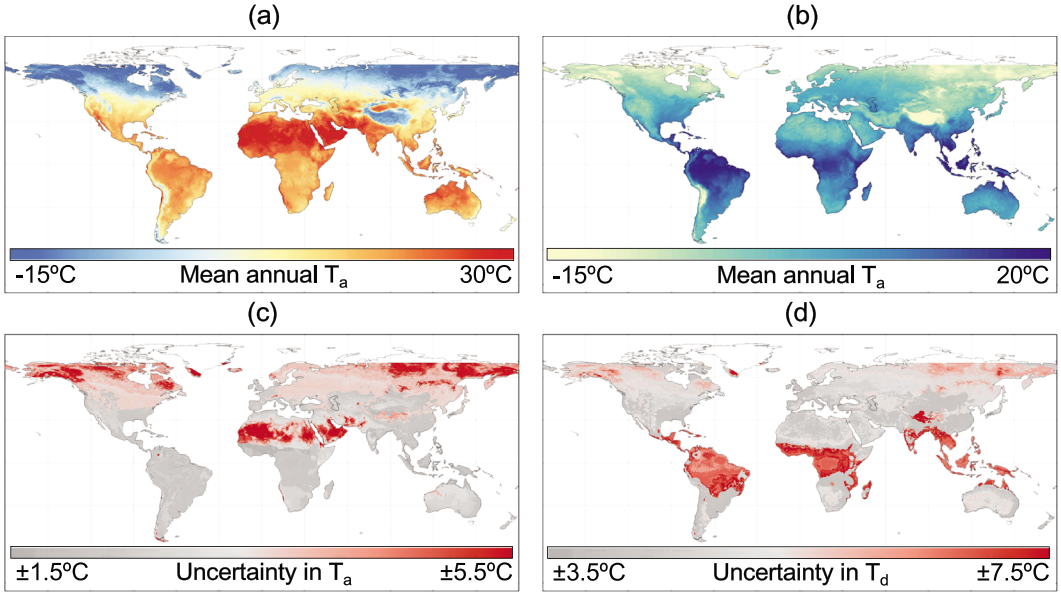

Figure 3. Regions of extreme annual mean (a) near-surface air temperature (T_a) or (b) dew point (T_d) correspond to high-magnitude uncertainties in MOD07-derived (c) T_a or (d) T_d estimates, respectively.

the difficulties of remote sensing in polar regions due to similarities of snow and clouds in the spectral bands. In their validation of another MODIS-derived land surface temperature product over the Peruvian Amazon, Gomis-Cebolla et al. (2018) applied alternative cloud filtering approaches to address such contamination. These improved product accuracy, but vastly reduced data volume. Chan and Comiso (2012) demonstrated significant inconsistencies in cloud detection capabilities dependent on surface type and solar illumination between the MODIS, Cloud-Aerosol Lidar with Orthogonal Polarization (CALIOP), and *CloudSat* Cloud Profiling Radar sensors. In their analysis of the ability of MOD07 to capture urban heat island dynamics, Hu and Brunsell (2015) named two factors causing unrealistic profiles: the presence of clouds and sharp changes in atmospheric structure. Furthermore, other studies analyzing the varying performance of MODIS products by climate have noted trends in statistical results analogous to ours. The validation of MOD16 global terrestrial evapotranspiration products by Kim et al. (2012), for instance, found the highest magnitudes of both bias and RMSE at their tropical sites and the weakest linear correlations at their two Arctic and arid sites.

Errors due to electronic crosstalk, in which signals from the detectors among the long-wave infrared photovoltaic bands leak to other detectors (Borbas et al., 2017), were minimized in this study due to processing updates introduced in Collection 6.1. The influence of crosstalk-related contamination in many Terra MODIS Level-2 products has increased over the mission lifetime (in particular, since 2010 for band 27 and since 2012 for bands 28 and 29; Wilson et al., 2016), causing inadvertent detector striping and increased radiometric bias that have compromised data quality. To offset these errors, a linear crosstalk correction algorithm was recently developed by the MODIS Characterization Support Team and adopted for implementation into Terra MODIS Collection 6.1 (Wilson et al., 2017), publically released in December 2017. We compared error dynamics over time for T_a and T_d data sets derived from both Collection 6.0 and Collection 6.1, the latter having been used in this study. Our results notably highlighted an increasing trend in error from 2011 onward in the Collection 6.0 T_a data that is absent in the Collection 6.1 variant for nearly all climate zones (Figures S9a–S9e), as well as similar bias offsets after 2010 for T_d (Figures S9f–S9j). Albeit minor, these improvements were consequential, and we encourage users to upgrade to Collection 6.1 when possible.

The representativeness of site measurements for MODIS pixels varies with land surface heterogeneity and has the capacity to skew results (Cescatti et al., 2012; Wang et al., 2008; Zhang et al., 2006). Solutions to the problem include attempts to upscale FLUXNET observations to the spatial scales of the remote sensing resolution, as well as careful selections of ground sites based on quantitative characterizations of their landscape homogeneity (Jung et al., 2011; Liang et al., 2002). However, many limitations associated with FLUXNET site-to-pixel

comparisons involve the spatial sensitivity of energy and mass fluxes between terrestrial ecosystems and the atmosphere (Baldocchi, 2003; Petropolous, 2014). In contrast, near-surface meteorology is captured far more reliably by ground stations (Simmons et al., 2004; Thornton et al., 1997). Indeed, the removal of three topographically heterogeneous ground locations that were initially included in our analyses decreased the average RMSE by only 0.11°C in the T_a data set and by 0.01°C in the T_d data set. We expect further amendments to our ground data sets based on heterogeneity to yield similarly negligible differences in statistical results.

Some trends in the errors we observed were anticipated. These include the larger errors on average obtained in the T_d data set than the T_a data set, as well as the more variable performance of MODIS T_d estimates in Arctic climates. Previous studies suggested the former. Using radiosonde data to validate the MOD07 profiles over the Iberian Peninsula, Sobrino et al. (2015) found larger bias and RMSE in dew point retrievals than in air temperature retrievals at multiple pressure levels, including the near-surface. Another example is work by Kim and Hogue (2008), which compared eight MODIS-derived variables including the MOD07 T_a and T_d to ground-based observations from four U.S. study sites. At all locations, the average RMSE in T_d measurements exceeded that in T_a estimates by at least 1.5 K. In their study of net radiation centered in the Southern Great Plains, Bisht and Bras (2010) found an average error in daytime MOD07 T_d estimates (6.08 K) of more than double that in T_a estimates (2.93 K). Our results align with these studies. Water vapor is notoriously difficult to capture because its concentration in the atmosphere is constantly fluctuating, making it more difficult to correct for in satellite observations than other measurements (Prince et al., 1998). Additionally, it has been well documented that humidity is challenging to measure under cold conditions, by both sounding instruments and radiosondes (Kwon et al., 2012; Miloshevich et al., 2001).

Finally, some applications requiring the MOD07 T_a and T_d may involve relative humidity (RH) calculations. Evapotranspiration products from both the Priestley-Taylor Jet Propulsion Laboratory (PT-JPL) algorithm and the Breathing Earth System Simulator (BESS) require a MODIS-derived RH estimate as input, for instance (Fisher et al., 2008; Ryu et al., 2011). Due to the amplification of seemingly insignificant errors carried through the conversion process, a comparison between MODIS-derived and FLUXNET-derived RH values is not straightforward. In particular, the remotely sensed RH product includes the compounded effects of errors associated with two distinct estimates (T_a and T_d). These issues are analogous to those experienced by Jolly et al. (2005) in their estimation via three tested interpolators of VPD, a quantity reliant on the same two conversion input variables as RH. Future studies or modeling efforts involving the MOD07-derived RH will likely benefit from the temporal aggregation of T_a and T_d measurements to superdaily timescales. This operation greatly reduces noise, and thereby error. In particular, aggregation from daily MODIS observations to their weekly averages decreased overall RMSE in both the T_a and T_d data sets by 17%. We observed still larger reductions at biweekly (22%, T_a; 23%, T_d) and monthly (25%, T_a; 24%, T_d) scales.

5. Conclusions

This study validated T_a and T_d estimates derived from the MOD07 Level-2 atmospheric profile product against data sampled from 109 geographically dispersed ground stations (FLUXNET) in six continents and all major Köppen-Geiger climate types, and is among the first assessments of the reprocessed, crosstalk-corrected Collection 6.1 Terra MODIS data. The daily MODIS-derived T_a and T_d estimates, hypsometrically interpolated to surface pressure level, were high in quality, marked by low bias and strong linear agreement between the satellite and in situ observations. We calculated mean RMSE's of 3.47 and 5.04°C in the T_a and T_d data sets, respectively. Although partitions based on climate type exposed variations in MODIS estimation accuracy, with relatively poor performance in Arctic regions, no differences in error obtained between climates were significant, implying that both remotely sensed temperature measurements are reliable and sufficiently precise on a global scale. The overall high accuracy of the MODIS-derived T_a and T_d will inform future modeling efforts involving either of the two quantities as input data.

Acknowledgments

This work used data acquired and shared by the FLUXNET community. The FLUXNET eddy covariance data processing and harmonization were carried out by the European Fluxes Database Cluster, AmeriFlux Management Project, and Fluxdata project of FLUXNET, with the support of CDIAC and ICOS Ecosystem Thematic Center, and the OzFlux, ChinaFlux, and AsiaFlux offices. Data from the MOD07 Level-2 atmospheric profile product are generated by the MODIS Adaptive Processing System (MODAPS) and the MODIS Atmosphere Science Team/Atmosphere Profile Retrieval Group. They are publicly available and can be obtained online (doi: 10.5067/MODIS/MOD07_L2.061). The authors thank J. C. Jiménez-Muñoz and one anonymous reviewer for their helpful comments and critiques. We also thank A. J. Purdy, E. Stofferahn, and J. S. Famiglietti for their contributions. The work was supported by funding from multiple NASA programs: THP, SUSMAP, IDS, INCA, and ECOSTRESS. The research was carried out at the Jet Propulsion Laboratory, California Institute of Technology, under a contract with the National Aeronautics and Space Administration California Institute of Technology. Government sponsorship acknowledged.

References

Arnold, J. G., Srinivasan, R., Muttiah, R. S., & Williams, J. R. (1998). Large area hydrologic modeling and assessment part I: Model development. *Journal of the American Water Resources Association*, *34*(1), 73–89. https://doi.org/10.1111/j.1752-1688.1998.tb05961.x

Aumann, H. H., Chahine, M. T., Gautier, C., Goldberg, M. D., Kalnay, E., McMillin, L. M., et al. (2003). AIRS/AMSU/HSB on the Aqua mission: Design, science objectives, data products, and processing systems. *IEEE Transactions on Geoscience and Remote Sensing*, *41*(2), 253–264. https://doi.org/10.1109/TGRS.2002.808356

Baldocchi, D. D. (2003). Assessing the eddy covariance technique for evaluating carbon dioxide exchange rates of ecosystems: Past, present and future. *Global Change Biology*, *9*(4), 479–492. https://doi.org/10.1046/j.1365-2486.2003.00629.x

Baldocchi, D. D., Falge, E., Gu, L., Olson, R., Hollinger, D. Y., Running, S., et al. (2001). FLUXNET: A new tool to study the temporal and spatial variability of ecosystem-scale carbon dioxide, water vapor, and energy flux densities. *Bulletin of the American Meteorological Society*, *82*(11), 2415–2434. https://doi.org/10.1175/1520-0477(2001)082%3C2415:FANTTS%3E2.3.CO;2

Bisht, G., & Bras, R. L. (2010). Estimation of net radiation from the MODIS data under all sky conditions: Southern Great Plains case study. *Remote Sensing of Environment*, *114*(7), 1522–1534. https://doi.org/10.1016/j.rse.2010.02.007

Bisht, G., Venturini, V., Islam, S., & Jiang, L. (2005). Estimation of the net radiation using MODIS (Moderate Resolution Imaging Spectroradiometer) data for clear sky days. *Remote Sensing of Environment*, *97*(1), 52–67. https://doi.org/10.1016/j.rse.2005.03.014

Bolton, D. (1980). The computation of equivalent potential temperature. *Monthly Weather Review*, *108*(7), 1046–1053. https://doi.org/10.1175/1520-0493(1980)108%3C1046:TCOEPT%3E2.0.CO;2

Borbas, E. E., Menzel, W. P., & Moeller, C. (2017). Collection 6.1 change document TERRA MOD07 atmospheric profile products. Retrieved from https://modis-atmosphere.gsfc.nasa.gov/sites/default/files/ModAtmo/MOD07_C61_ChangeDoc.pdf

Borbas, E. E., Seemann, S. W., Kern, A., Moy, L., Li, J., Gumley, L., & Menzel, W. P. (2011). MODIS atmospheric profile retrieval algorithm theoretical basis document. Retrieved from https://modis-atmos.gsfc.nasa.gov/_docs//MOD07_atbd_v7_April2011.pdf

Brun, E., Martin, E., Simon, V., Gendre, C., & Coleou, C. (1989). An energy and mass model of snow cover suitable for operational avalanche forecasting. *Journal of Glaciology*, *35*(121), 333–342. https://doi.org/10.1017/S0022143000009254

Cescatti, A., Marcolla, B., Santhana Vannan, S. K., Pan, J. Y., Román, M. O., Yang, X., et al. (2012). Intercomparison of MODIS albedo retrievals and in situ measurements across the global FLUXNET network. *Remote Sensing of Environment*, *121*, 323–334. https://doi.org/10.1016/j.rse.2012.02.019

Chan, M. A., & Comiso, J. C. (2012). Arctic cloud characteristics as derived from MODIS, CALIPSO, and CloudSat. *Journal of Climate*, *26*(10), 3285–3306. https://doi.org/10.1175/JCLI-D-12-00204.1

Dee, D. P., Uppala, S. M., Simmons, A. J., Berrisford, P., Poli, P., Kobayashi, S., et al. (2011). The ERA-Interim reanalysis: Configuration and performance of the data assimilation system. *Quarterly Journal of the Royal Meteorological Society*, *137*(656), 553–597. https://doi.org/10.1002/qj.828

Fisher, J. B., Tu, K. P., & Baldocchi, D. D. (2008). Global estimates of the land-atmosphere water flux based on monthly AVHRR and ISLSCP-II data, validated at 16 FLUXNET sites. *Remote Sensing of Environment*, *112*(3), 901–919. https://doi.org/10.1016/j.rse.2007.06.025

Fluxdata (2016). FLUXNET2015 Dataset. Retrieved from http://fluxnet.fluxdata.org/data/fluxnet2015-dataset/

Gelaro, R., McCarty, W., Suárez, M. J., Todling, R., Molod, A., Takacs, L., et al. (2017). The Modern-Era Retrospective Analysis for Research and Applications, Version 2 (MERRA-2). *Journal of Climate*, *30*(14), 5419–5454. https://doi.org/10.1175/JCLI-D-16-0758.1

Gomis-Cebolla, J., Jimenez, J. C., & Sobrino, J. A. (2018). LST retrieval algorithm adapted to the Amazon evergreen forests using MODIS data. *Remote Sensing of Environment*, *204*, 401–411. https://doi.org/10.1016/j.rse.2017.10.015

Harris, I., Jones, P. D., Osborn, T. J., & Lister, D. H. (2014). Updated high-resolution grids of monthly climatic observations—The CRU TS3.10 dataset. *International Journal of Climatology*, *34*(3), 623–642. https://doi.org/10.1002/joc.3711

Hu, L., & Brunsell, N. A. (2015). A new perspective to assess the urban heat island through remotely sensed atmospheric profiles. *Remote Sensing of Environment*, *158*, 393–406. https://doi.org/10.1016/j.rse.2014.10.022

Hubanks, P. (2017). MODIS atmosphere QA plan for Collection 061. Retrieved from https://modis-atmosphere.gsfc.nasa.gov/sites/default/files/ModAtmo/QA_Plan_C61_Master_2017_03_15.pdf

Hubbard, K., Mahmood, R., & Carlson, C. (2003). Estimating daily dew point temperature for the Northern Great Plains using maximum and minimum temperature. *Agronomy Journal*, *95*(2), 323–328. https://doi.org/10.2134/agronj2003.0323

Jiménez-Muñoz, J. C., Sobrino, J. A., Mattar, C., & Franch, B. (2010). Atmospheric correction of optical imagery from MODIS and reanalysis atmospheric products. *Remote Sensing of Environment*, *114*(10), 2195–2210. https://doi.org/10.1016/j.rse.2010.04.022

Jolly, W. M., Graham, J. M., Michaelis, A., Nemani, R., & Running, S. W. (2005). A flexible, integrated system for generating meteorological surfaces derived from point sources across multiple geographic scales. *Environmental Modelling & Software*, *20*(7), 873–882. https://doi.org/10.1016/j.envsoft.2004.05.003

Jung, M., Reichstein, M., Margolis, H. A., Cescatti, A., Richardson, A. D., Arain, M. A., et al. (2011). Global patterns of land-atmosphere fluxes of carbon dioxide, latent heat, and sensible heat derived from eddy covariance, satellite, and meteorological observations. *Journal of Geophysical Research*, *116*, G00J07. https://doi.org/10.1029/2010JG001566

Kalnay, E., Kanamitsu, M., Kistler, R., Collins, W., Deaven, D., Gandin, L., et al. (1996). The NCEP/NCAR 40-Year Reanalysis Project. *Bulletin of the American Meteorological Society*, *77*(3), 437–471. https://doi.org/10.1175/1520-0477(1996)077%3C0437:TNYRP%3E2.0.CO;2

Kim, H. W., Hwang, K., Mu, Q., Lee, S. O., & Choi, M. (2012). Validation of MODIS 16 global terrestrial evapotranspiration products in various climates and land cover types in Asia. *KSCE Journal of Civil Engineering*, *16*(2), 229–238. https://doi.org/10.1007/s12205-012-0006-1

Kim, J., & Hogue, T. S. (2008). Evaluation of a MODIS-based potential evapotranspiration product at the point scale. *Journal of Hydrometeorology*, *9*(3), 444–460. https://doi.org/10.1175/2007JHM902.1

King, M. D., Menzel, W. P., Kaufman, Y. J., Tanre, D., Gao, B.-C., Platnick, S., et al. (2003). Cloud and aerosol properties, precipitable water, and profiles of temperature and water vapor from MODIS. *IEEE Transactions on Geoscience and Remote Sensing*, *41*(2), 442–458. https://doi.org/10.1109/TGRS.2002.808226

Kite, G. W., & Droogers, P. (2000). Comparing evapotranspiration estimates from satellites, hydrological models and field data. *Journal of Hydrology*, *229*(1-2), 3–18. https://doi.org/10.1016/S0022-1694(99)00195-X

Kwon, E.-H., Sohn, B. J., Smith, W. L., & Li, J. (2012). Validating IASI temperature and moisture sounding retrievals over East Asia using radiosonde observations. *Journal of Atmospheric and Oceanic Technology*, *29*(9), 1250–1262. https://doi.org/10.1175/JTECH-D-11-00078.1

Liang, S., Fang, H., Chen, M., Shuey, C. J., Walthall, C., Daughtry, C., et al. (2002). Validating MODIS land surface reflectance and albedo products: Methods and preliminary results. *Remote Sensing of Environment*, *83*(1-2), 149–162. https://doi.org/10.1016/S0034-4257(02)00092-5

Loveland, T. R., Brown, J., Ohlen, D., Reed, B., Zhu, Z., Yang, L., & Howard, S. (2009). ISLSCP II IGBP DISCover and SiB land cover, 1992–1993. ORNL Distributed Active Archive Center. https://doi.org/10.3334/ornldaac/930

Miloshevich, L. M., Vömel, H., Paukkunen, A., Heymsfield, A. J., & Oltmans, S. J. (2001). Characterization and correction of relative humidity measurements from Vaisala RS80—A radiosondes at cold temperatures. *Journal of Atmospheric and Oceanic Technology*, *18*(2), 135–156. https://doi.org/10.1175/1520-0426(2001)018%3C0135:CACORH%3E2.0.CO;2

Østby, T. I., Schuler, T. V., & Westermann, S. (2014). Severe cloud contamination of MODIS land surface temperatures over an Arctic ice cap, Svalbard. *Remote Sensing of Environment*, *142*, 95–102. https://doi.org/10.1016/j.rse.2013.11.005

Peel, M. C., Finlayson, B. L., & McMahon, T. A. (2007). Updated world map of the Köppen-Geiger climate classification. *Hydrology and Earth System Sciences*, *11*(5), 1633–1644. https://doi.org/10.5194/hess-11-1633-2007

Penman, H. L. (1948). Natural evaporation from open water, bare soil and grass. *Proceedings of the Royal Society of London. Series A: Mathematical and Physical Sciences*, *193*(1032), 120 LP-145. Retrieved from http://rspa.royalsocietypublishing.org/content/193/1032/120.abstract

Petropolous, G. P. (2014). *Remote sensing of energy fluxes and soil moisture content*. Boca Raton: CRC Press.

Prince, S. D., Goetz, S. J., Dubayah, R. O., Czajkowski, K. P., & Thawley, M. (1998). Inference of surface and air temperature, atmospheric precipitable water and vapor pressure deficit using Advanced Very High-Resolution Radiometer satellite observations: Comparison with field observations. *Journal of Hydrology*, *212-213*, 230–249. https://doi.org/10.1016/S0022-1694(98)00210-8

Rehman, S., & Mohandes, M. (2008). Artificial neural network estimation of global solar radiation using air temperature and relative humidity. *Energy Policy*, *36*(2), 571–576. https://doi.org/10.1016/j.enpol.2007.09.033

Ryu, Y., Baldocchi, D. D., Kobayashi, H., van Ingen, C., Li, J., Black, T. A., et al. (2011). Integration of MODIS land and atmosphere products with a coupled-process model to estimate gross primary productivity and evapotranspiration from 1 km to global scales. *Global Biogeochemical Cycles*, *25*, GB4017. https://doi.org/10.1029/2011GB004053

Seemann, S. W., Li, J., Menzel, W. P., & Gumley, L. (2003). Operational retrieval of atmospheric temperature, moisture, and ozone from MODIS infrared radiances. *Journal of Applied Meteorology*, *42*(8), 1072–1091. https://doi.org/10.1175/1520-0450(2003)042%3C1072:OROATM%3E2.0.CO;2

Sellers, P. J., Dickinson, R. E., Randall, D. A., Betts, A. K., Hall, F. G., Berry, J. A., et al. (1997). Modeling the exchanges of energy, water, and carbon between continents and the atmosphere. *Science*, *275*(5299), 502–509. https://doi.org/10.1126/science.275.5299.502

Simmons, A. J., Jones, P. D., da Costa Bechtold, V., Beljaars, A. C. M., Kållberg, P. W., Saarinen, S., et al. (2004). Comparison of trends and low-frequency variability in CRU, ERA-40, and NCEP/NCAR analyses of surface air temperature. *Journal of Geophysical Research*, *109*, D24115. https://doi.org/10.1029/2004JD005306

Sobrino, J. A., Jiménez-Muñoz, J. C., Mattar, C., & Sòria, G. (2015). Evaluation of Terra/MODIS atmospheric profiles product (MOD07) over the Iberian Peninsula: A comparison with radiosonde stations. *International Journal of Digital Earth*, *8*(10), 771–783. https://doi.org/10.1080/17538947.2014.936973

Thornton, P. E., Running, S. W., & White, M. A. (1997). Generating surfaces of daily meteorological variables over large regions of complex terrain. *Journal of Hydrology*, *190*(3–4), 214–251. https://doi.org/10.1016/S0022-1694(96)03128-9

Verma, M., Fisher, J., Mallick, K., Ryu, Y., Kobayashi, H., Guillaume, A., et al. (2016). Global surface net-radiation at 5 km from MODIS Terra. *Remote Sensing*, *8*(9), 739. https://doi.org/10.3390/rs8090739

Wan, Z., Zhang, Y., Zhang, Q., & Li, Z. (2002). Validation of the land-surface temperature products retrieved from Terra Moderate Resolution Imaging Spectroradiometer data. *Remote Sensing of Environment*, *83*(1), 163–180. https://doi.org/10.1016/S0034-4257(02)00093-7

Wang, W., Liang, S., & Meyers, T. (2008). Validating MODIS land surface temperature products using long-term nighttime ground measurements. *Remote Sensing of Environment*, *112*(3), 623–635. https://doi.org/10.1016/j.rse.2007.05.024

Wilson, T., Wu, A., Geng, X., Wang, Z., & Xiong, X. (2016). Analysis of the electronic crosstalk effect in Terra MODIS long-wave infrared photovoltaic bands using lunar images (Vol. 10004, 15 pp.). https://doi.org/10.1117/12.2240574

Wilson, T., Wu, A., Shrestha, A., Geng, X., Wang, Z., Moeller, C., et al. (2017). Development and implementation of an electronic crosstalk correction for bands 27–30 in Terra MODIS Collection 6. *Remote Sensing*, *9*(6). https://doi.org/10.3390/rs9060569

Wood, E. F., Roundy, J. K., Troy, T. J., van Beek, L. P. H., Bierkens, M. F. P., Blyth, E., et al. (2011). Hyperresolution global land surface modeling: Meeting a grand challenge for monitoring Earth's terrestrial water. *Water Resources Research*, *47*, W05301. https://doi.org/10.1029/2010WR010090

Zhang, H., Wu, B., Yan, N., Zhu, W., & Feng, X. (2014). An improved satellite-based approach for estimating vapor pressure deficit from MODIS data. *Journal of Geophysical Research: Atmospheres*, *119*, 12,256–12,271. https://doi.org/10.1002/2014JD022118

Zhang, X., Friedl, M. A., & Schaaf, C. B. (2006). Global vegetation phenology from Moderate Resolution Imaging Spectroradiometer (MODIS): Evaluation of global patterns and comparison with in situ measurements. *Journal of Geophysical Research*, *111*, G04017. https://doi.org/10.1029/2006JG000217

Zhu, W., Lű, A., Jia, S., Yan, J., & Mahmood, R. (2017). Retrievals of all-weather daytime air temperature from MODIS products. *Remote Sensing of Environment*, *189*, 152–163. https://doi.org/10.1016/j.rse.2016.11.011